**Quantitative observations and numerical modeling of charge development in volcanic eruption clouds**

Andre Geisler[1], Benjamin Seelmann[2], Matthias Hort[3], Michael Herzog[4], Jack Atkinson[4], Joachim Bülow[2], Lea Scharff[2], Masato Iguchi[5], and Daisuke Miki[5]

- Installation of a multiparameter geophysical network at Sakurajima Volcano, Japan
  - Defining an event catalog from infrasound and radar data as well as a video camera and local authorities[6]
  - Lightning detection by field mills and thunderstorm detector
  - Characterizing eruption conditions with network data
- Numerical modelling of charge build-up using an eruption column model
  - Compare results to field measurements

[1]University of Hamburg, andre.geisler@uni-hamburg.de
[2]University of Hamburg
[3]University of Hamburg, matthias.hort@uni-hamburg.de
[4]University of Cambridge
[5]Sakurajima Volcano Research Center, Disaster Prevention Research Institute, Kyoto University
[6]Japanese Meteorological Agency (JMA) and Tokyo Volcanic Ash Advisory Center (VAAC)

# 1 Network

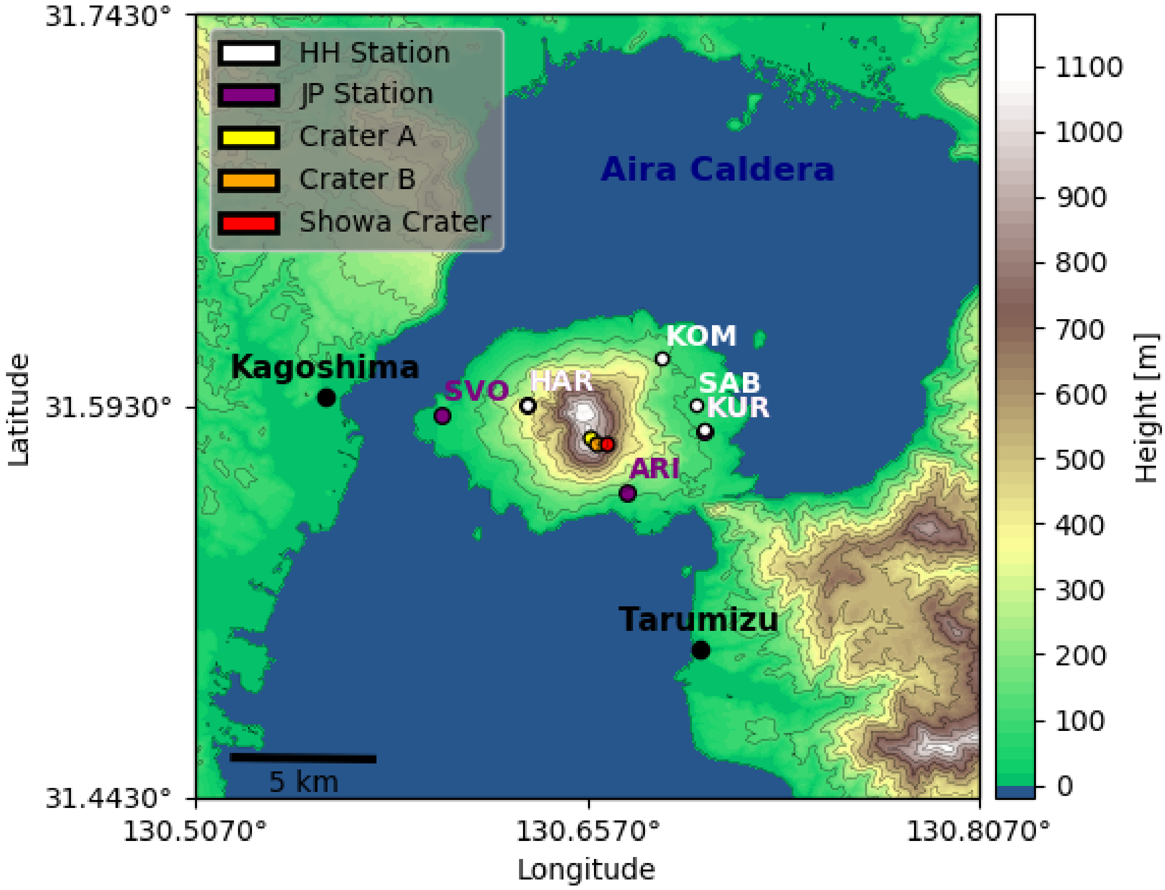


*Figure 1.1: Station locations of the network. White: stations installed by Hamburg University. Purple: acoustic stations of Sakurajima Volcano Observatory (SVO). There are white and purple markers at locations "HAR" and "KUR".*

*Table 1.1: Instruments of the network.*

| Instrument | Observation | Locations |
|---|---|---|
| Electric field mills (3) | eletric field | HAR, KOM and KUR |
| Thunderstorm detector | electric field change | HAR |
| Weather station | meteorological conditions | KUR |
| Doppler radar systems (3) | ejected particles | KUR |
| Infrasound sensor* | acoustic emissions | KOM |
| Seismometer | acoustic emissions | KOM |
| Camera | visual | KUR |

*Infrasound network is complemented by four Japanese stations (SVO, HAR, ARI, KUR)

# 2 Event Catalog

Fig. 2.1 shows different event catalogs. Each line represents an interval in which an event occured. The events shown range from small ash ejections/ash venting to eruption columns with up to 5 km height.

- Event catalogs derived from network data and local authorities
- An event might be divied into individual pulses (separate lines in Fig. 2.1)
- The network identifies significantly more eruptions than local authorities report
- Catalogs used for further investigation

*Table 2.1: Generation of the event catalogs from different data sets.*

| | Event detection | | #events |
|---|---|---|---|
| Instrument | Method | Remarks | Fig. 2.1 |
| Infrasound | STA/LTA | - includes japanese stations<br>- resolution: a few tens of seconds | 195 |
| Radar | hand picked | - results from radar aligned at crater A<br>- resolution: a few seconds | 306 |
| Camera | hand picked | - results limited by sight of crater region (e.g. daytime and clouds)<br>- resolution: one minute (with limited sight worse) | 132 |
| JMA | n.a. | - no report of small eruptions<br>- time sometimes a little of during continuous ash venting<br>- resolution: one minute | 80 |
| VAAC | satellite | - HIMAWARI-8 images<br>- resolution: images every 10 minutes, eruption times 1 minute (from JMA) | 56 |

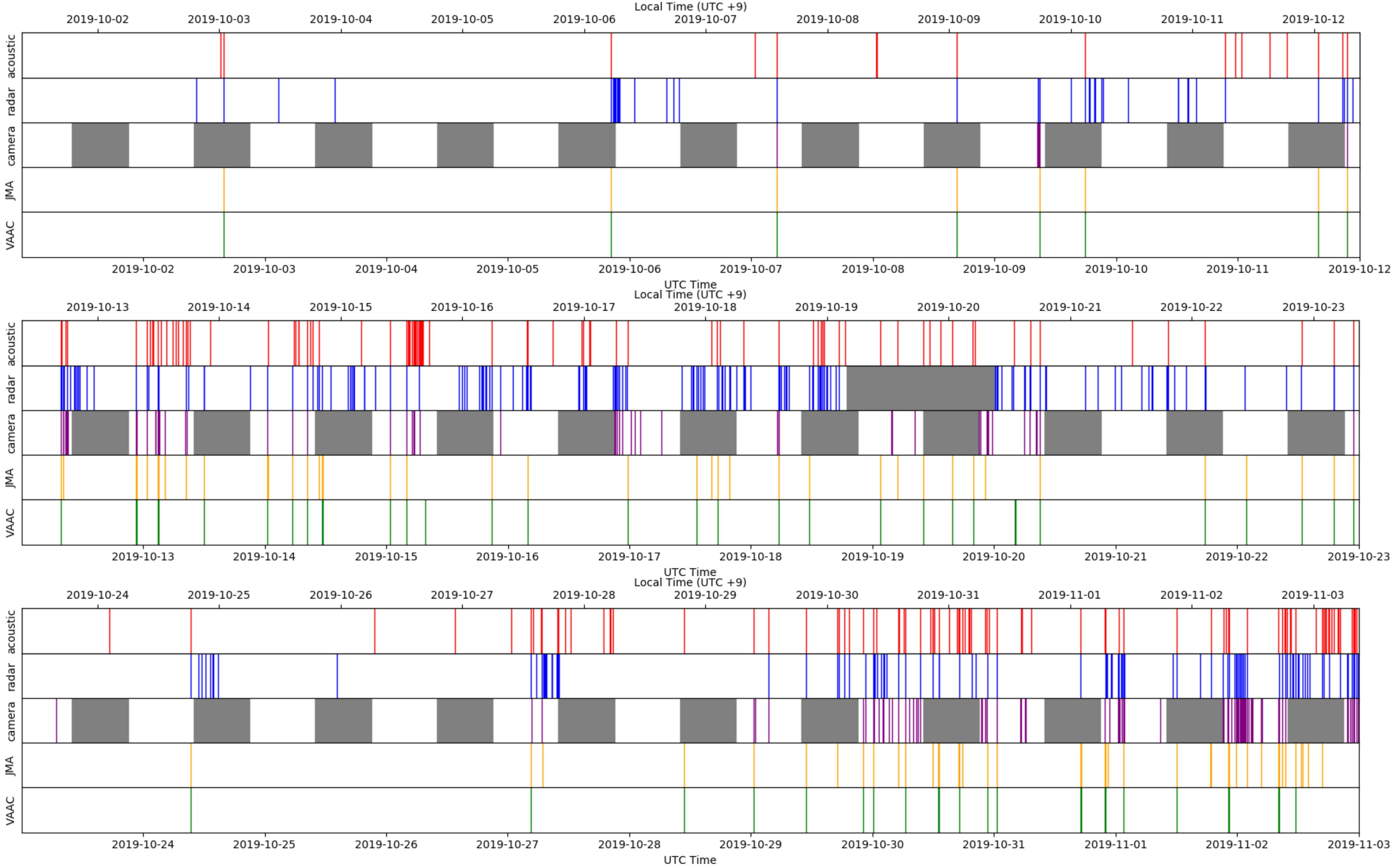


*Figure 2.1: Comparison of the different event catalogs. Times when no data were recorded are marked grey. Each line represents an individual event. For events seperated by a few minutes the resolution will result in a thicker line.*

# 3 Electrical Charging

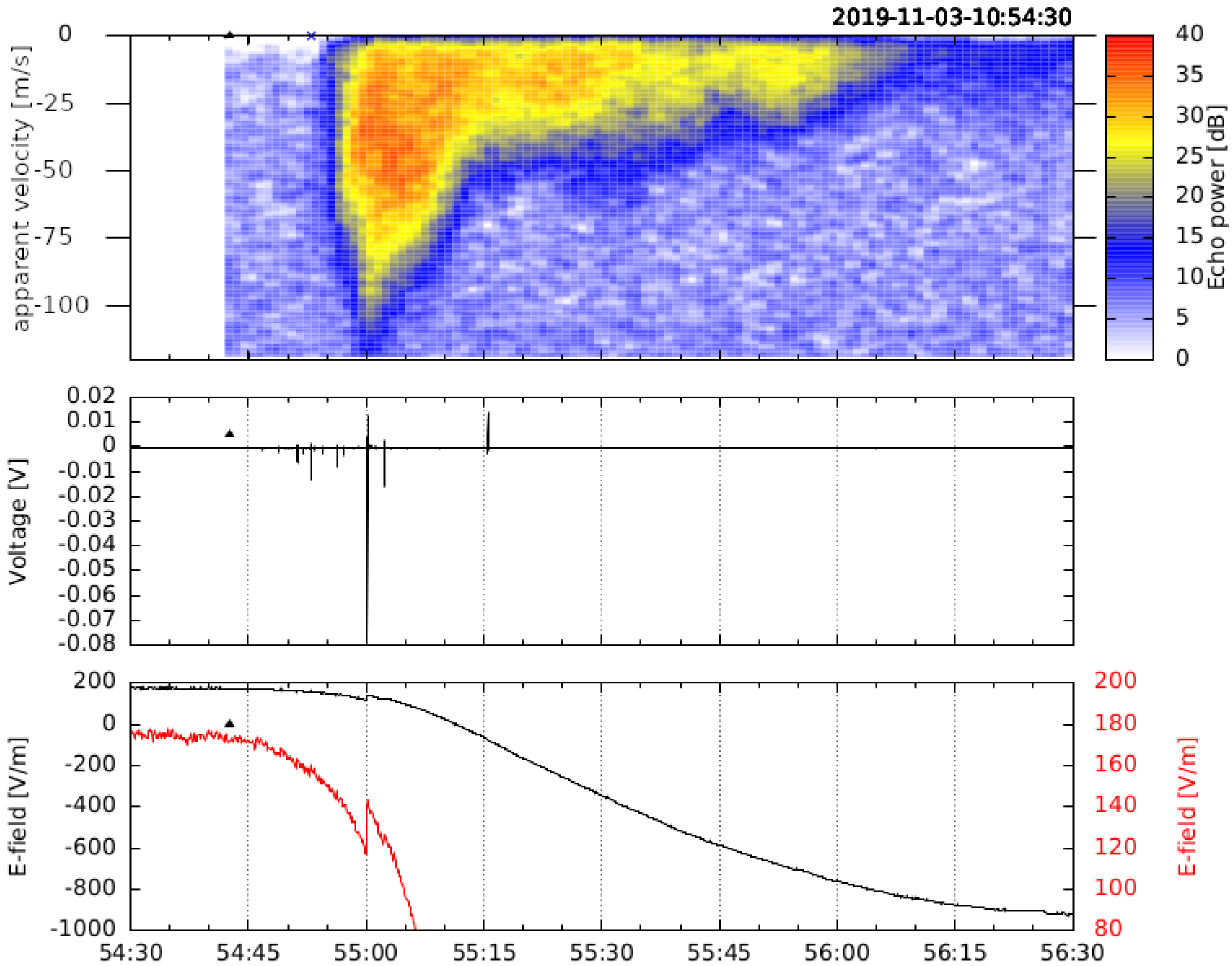


*Figure 3.1: Data from an eruption on November 3rd at 10:54 UTC. Eruption onsets as defined by the acoustic network (black triangle) and by the radar (blue cross). (a): Radar-"velocigram" for ascending particles. Reflected energy (color coded* [dB]*) from particles with different apparent ascent velocities (y-axis* [m/s]*) within the eruption column. (b): Induced voltage by sudden changes in electric field in the thunderstorm detector (BTD300). (c): Electric field as measured by a field mill about* 3 km *away from the crater.*

- Small eruption (not reported by JMA and VAAC)
- With eruption onset electric field starts decreasing due to charged particles within the eruption column (fracto- or triboelectrification)
- Peaks in the thunderstorm data coincide with jumps in field mill data and correspond to discharges
- First discharges occur just a few seconds after the eruption onset
- Strongest discharges occur in times of highest particle velocities and highest reflected energies

# 4 Numerical modeling

- Calculating ash concentrations for a discrete particle size distribution
- Assuming a fixed specific charge density for different particle sizes to calculate a charge distribution
  - For the moment charge is assumed to be generated within the conduit by fractoelectrification
- Solve poisson equation to calculate electric field

- Even with such a simple model approach the temporal evolution of the electric field observed in different locations on the ground is qualitative quite well matched by the numerical results (compare Fig. 4.1 and 4.2).
- Electric field pertubations are accompanied by dynamic processes in the eruption column

**Not included in the calculations:**

- Charge generation by triboelectrification
- Charge neutralization
- Electric discharges

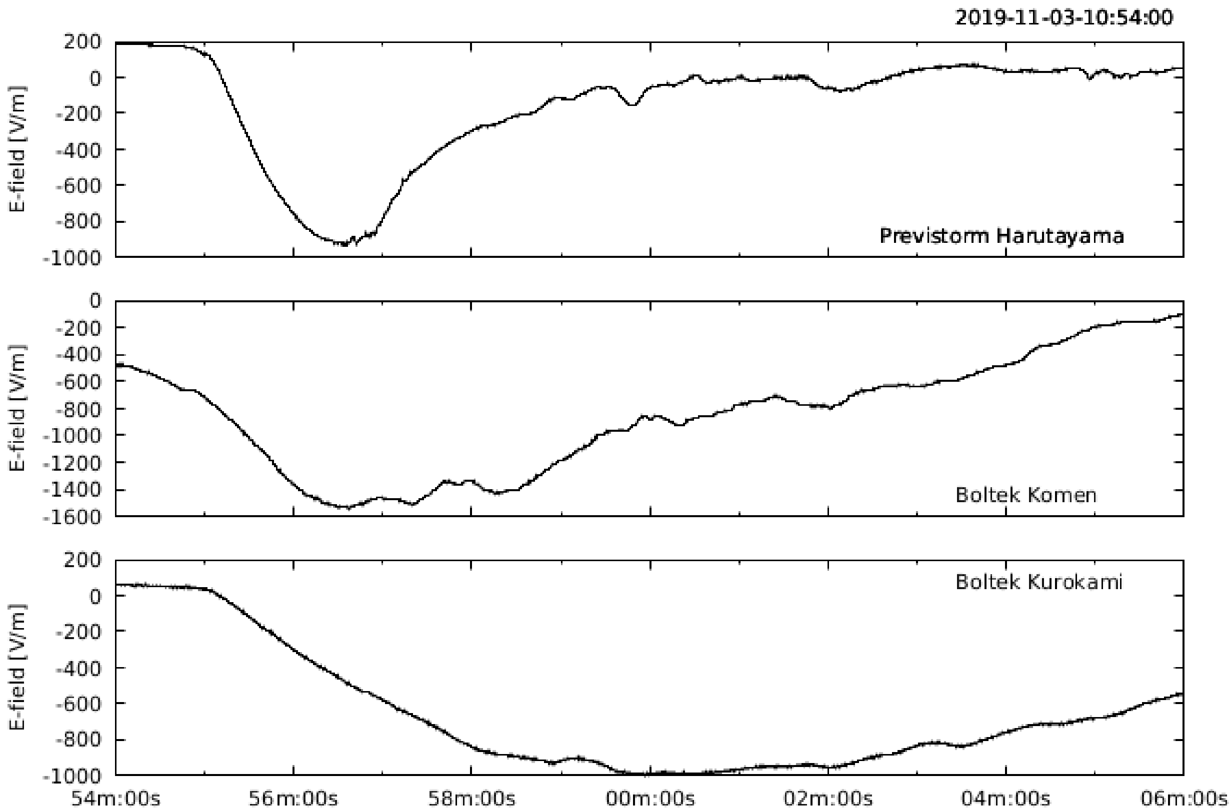


*Figure 4.1: Electric field pertubations measured by the three field mills at different stations for an eruption on November 3rd at 10:54 UTC. Distances are about* 3 km *for Harutayama and about* 4 km *for Komen and Kurokami.*

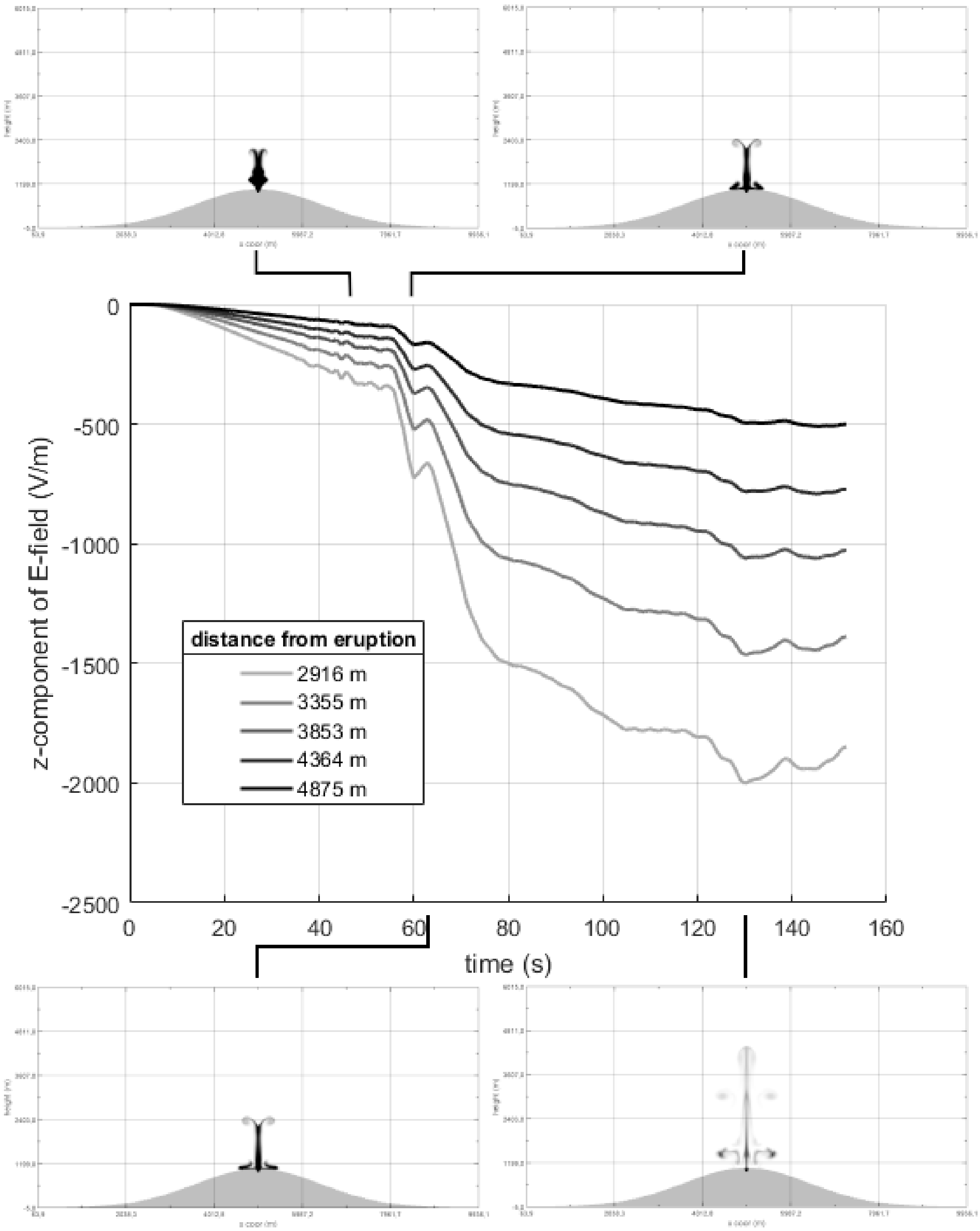


*Figure 4.2: Electric field strength calculated from the ash distribution. Ash distribution for different time steps.*

## 5 Conclusions

- The network identifies significantly more eruptions than officially reported by JMA and VAAC. Main reasons for this are the criteria for official reports.
- Charge is built-up with the eruption onset (before any ice/precipitation particles could possibly form)
- First electrical discharges occur a few seconds after eruption onset
- A first simple modelling approach can reproduce similar electric field fluctuations as measured in the field

## Acknowledgements

Collaboration in the field:
Caron Vossen and Corrado Cimarelli

This work is funded by the Deutsche Forschungsgemeinschaft (DFG) through grant Ho1411 26-1.